DOI 10.33111/nfmte.2021.003

IDENTIFYING STOCK MARKET CRASHES BY FUZZY MEASURES OF COMPLEXITY

Andrii Bielinskyi

Kryvyi Rih State Pedagogical University
54 Gagarin Ave., Kryvyi Rih, 50086, Ukraine
ORCID: 0000-0002-2821-2895, E-mail: krivogame@gmail.com

Vladimir Soloviev

Kryvyi Rih State Pedagogical University
54 Gagarin Ave., Kryvyi Rih, 50086, Ukraine
ORCID: 0000-0002-4945-202X, E-mail: vnsoloviev2016@gmail.com

Serhiy Semerikov

Kryvyi Rih State Pedagogical University
54 Gagarin Ave., Kryvyi Rih, 50086, Ukraine
ORCID: 0000-0003-0789-0272, E-mail: semerikov@gmail.com

Viktoria Solovieva

State University of Economics and Technology
16 Medychna Str., Kryvyi Rih, 50005, Ukraine
ORCID: 0000-0002-8090-9569, E-mail: vikasolovieva2027@gmail.com

This study, for the first time, presents the possibility of using fuzzy set theory in combination with information theory and recurrent analysis to construct indicators (indicators-precursors) of crisis phenomena in complex nonlinear systems. In our study, we analyze the 4 most important crisis periods in the history of the stock market – 1929, 1987, 2008 and the COVID-19 pandemic in 2020. In particular, using the sliding window procedure, we analyze how the complexity of the studied crashes changes over time, and how it depends on events such as the global stock market crises. For comparative analysis, we take classical Shannon entropy, approximation and permutation entropy, recurrent diagrams, and their fuzzy alternatives. Each of the fuzzy modifications uses three membership functions: exponential, sigmoidal, and simple linear functions. Empirical results demonstrate the fact that the fuzzification of classical entropy and recurrence approaches opens up prospects for constructing effective and reliable indicators-precursors of critical events in the studied complex systems.

Keywords: *crash, critical event, stock market, entropy, recurrence plot, fuzzy set theory, indicator-precursor of crisis phenomena, fuzzy measure of complexity*

JEL Classification: C22, C58, G01, G17

Introduction

Financial systems are complex, nonlinear, and nonstationary partially due to the plurality of trading agents that work either independently or interact with each other and form multiple subsystems. The evolution of a market is reflected in their cooperation that is based on a set of nonlinear rules and reflected in temporal and spatial structures at different scales [12].

The stock market system also has complex dynamical behavior and nonlinear characteristics. The nonlinear and nonstationary information hidden in the stock indices signals cannot be obtained by traditional linear methods [92]. Nonlinear measures may provide valuable insights in addition to the time- and frequency-domain features by evaluating the complexity or irregularity of time series [47]. Great attention has gained the studies devoted to the nonlinear complex dynamical systems, which has resulted in the development of concepts and methods devoted to fractal dimensions [28, 35, 51], bifurcations [16, 25, 68], and strange attractors [19, 29, 30, 74, 79]. While different interpretations of complexity may be assumed, entropy and recurrence analysis certainly play a role in the estimation of time series complexity and predictability. One of the most commonly used informational measures of complexity are approximate entropy (ApEn) [64], sample entropy (SampEn) [71], fuzzy entropy (FuzzyEn) [14, 96, 97], conditional entropy [80], distribution entropy [47], and permutation entropy (PEn) [7].

Great perspectives here present the concept of fuzzy sets in the combination with the information theory and recurrence analysis.

The concept of fuzzy set entropy was first introduced by De Luca and Termini [17], which defined entropy as “measuring the degree of ambiguity in a generalized set”. This definition of fuzzy entropy is different from the definition of Shannon entropy and its inheritors – Approximate and Sample entropies.

In the ApEn and the SampEn algorithms, the similarity of embedded vectors is based on the Heaviside function [71], which can

be considered as a two-state classification. However, the boundaries of the real-world systems can be ambiguous, making it difficult to determine if an input pattern belongs to a specific class [99]. Moreover, both the ApEn and the SampEn give unreliable or undefined results for short signals [6, 47, 73]. To overcome these shortcomings of the SampEn, fuzzy sets and fuzzy entropy (FuzzEn) based on the concept of the ApEn and the SampEn [14] were introduced. The fuzzy membership function shows that continuous boundaries guarantee continuity. The FuzzEn was found to be relatively consistent and less dependent on data length [15]. Therefore, the FuzzEn approach has been used in a variety of real-world applications, from neuroscience and biomedical engineering [14, 32, 69, 97] to engineering and financial research [2, 38, 46, 93, 94, 103, 108].

Another type of information entropy was proposed by Bandt and Pompe which is called permutation entropy [7]. This approach relies on the ordinal structure of a time series, deriving the average amount of information from the constructed patterns. The problem with the classic PEn is that it neglects the amplitude of a time series, sensitive to the choice of the embedding dimension and time delay as the previous two entropies. Also, its multiscale version needs long time series because of the procedure of coarse-graining [34]. Thus, to overcome such issues, the fuzzy permutation entropy (FuzzPEn) was proposed [102], considering it to be robust to noise and suitable for short time segments.

The concept of recurrence plots was introduced by Eckmann, Kamphorst, and Ruelle [20]. The idea behind their approach was to give a new graphical representation of the recurrence states of a dynamical system and capture essential features of its structure. Since the recurrence plot can be easily constructed and, on its basis, can be derived different quantitative measures of complexity and chaos such as the Lyapunov exponent [39], information and correlation dimension [23, 29], and other measures of recurrence quantification analysis [53, 81, 95], it has been wildly applied within different fields of science: neuroscience [1], finance [8, 90], cognitive science [18, 70], materials science [21, 24, 31, 33, 37, 72], atmospheric science [22, 48, 52, 88, 109], anthropology [40], engineering [50, 67, 89,

106], music [54, 76], dynamical systems theory [55, 56, 100, 101, 105], network traffic classification [57], cryptography [98].

The particular problem with the recurrence plots is the threshold selection. Like with the ApEn or the SampEn, the graphical representation of RP is sensitive to this parameter. Pham proposed to measure the similarity between two phase-space states through fuzzy c-means clustering that produces membership grades ranging between zero and one [58, 62]. Such an approach can not only solve the problem of threshold selection but also improve system dynamics visualization.

For the last decades, these methods have been extensively applied to various disciplines of econophysics [4, 36, 43, 44, 78] and financial phenomena [5, 8, 41, 42, 45, 90, 104, 107]. Therefore, this paper applies classic and fuzzy-based complexity indicators to the price sequence of the stock market index represented by the Dow Jones Industrial Average (DJIA) index for monitoring the developments of its unpredictability or complexity across time. In our study, we analyze the four most important crash periods in the history of the stock market with the classic entropy methods, recurrence plots, and their fuzzy-based analogs. In addition, using the sliding time window analysis, we observed how the complexity of the studied crashes changes with time. Indicators (indicators-precursors) of crisis phenomena are promising here, not only for ordinary stock market traders, but also for the global policymakers who will be able to find it extremely important to make decisions for the short, mid, and long-term, recognizing the increase in complexity in the market promptly.

Materials and Methods

To compare the classic information and recurrent methods with the fuzzified ones and to present indicators (indicators-precursors) of the crashes in the stock market, we have chosen four major crisis events of 1929, 1987, 2008, and 2020 years relying on the list of stock market crashes and bear markets provided in [49]. The sub-series of crashes were obtained from the daily data of the DJIA index.

Most of the studied measures are calculated regarding the standardized returns of the corresponding crash events, where returns are calculated as

$$G(t) = \ln x(t + \Delta t) - \ln x(t) \cong [x(t + \Delta t) - x(t)]/x(t), \quad (1)$$

and their standardized version can be obtained as

$$g(t) \cong [G(t) - \langle G \rangle]/\sigma, \quad (2)$$

with $\langle \cdot \rangle$ corresponding to the mean value and σ to the standard deviation of G.

During our experiments, we have found that

- standard Shannon, approximate, and their fuzzy analogs give the best results for the standardized returns;
- standard permutation entropy and its fuzzy analog represent the most robust results for the initial time series;
- standard recurrence plots give the clearest representation of the recurrent nature of crash events for the standardized variant of the initial time series. Fuzzy recurrence plots do not strictly depend on the initial representation of the studied system, i.e., your fuzzy recurrence diagram will be approximately the same whether you calculate it for the initial time series, its standardized representation, or returns.

All calculations that are performed in this study are realized in the web-interactive computational environment called Jupyter Notebook. The corresponding Jupyter document is realized with the Python programming language. The "Entropy Hub" package [27] served as the basis for the implementation of some types of entropy. All time series and the implemented program are freely available at [26].

Each of the presented methods except Shannon entropy relies on the phase-space reconstruction approach described by Takens' embedding theorem [91].

The presented fuzzified entropies use such membership functions as

- the exponential fuzzy function (default):

$$\mu(x, r_1, r_2) = \exp\left(-\frac{x^{r_2}}{r_1}\right), \quad (3)$$

where r_1 and r_2 are the width and gradient of the boundary of the fuzzy function;

- the sigmoid fuzzy function (sigmoid):

$$\mu(x, r_1, r_2) = \frac{1}{1 + \exp\left(\frac{x - r_2}{r_1}\right)}; \quad (4)$$

- the linear fuzzy function (linear) according to [27]:

$$\mu(x) = \exp\left(-(x - x_{\min})\right). \quad (5)$$

For both exponential and sigmoid membership functions were tested different parameters r_1 and r_2. During experiments we have found that $r_1 = 0.45$ and $r_2 = 2.0$ give reasonable and robust results. However, further experiments may be carried out.

Fig. 1. represents the dependence of the presented fuzzy functions on different *x*-values with the predefined parameters r_1 and r_2 for default and sigmoid functions.

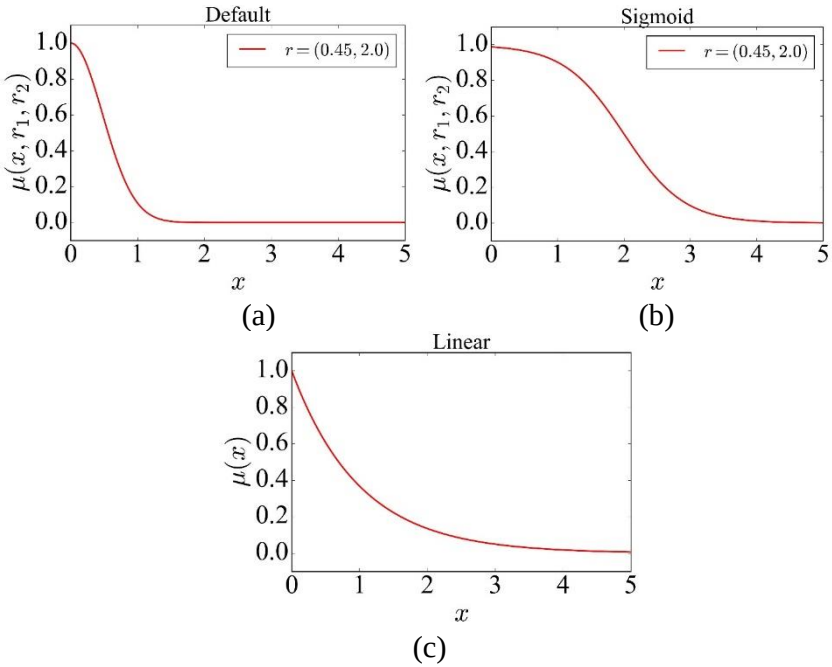

Fig. 1. The dependence of default (a), sigmoid (b), and linear (c) membership functions on different *x*-values

From Fig. 1 we can see that the highest membership degree is expectable for x-values with the closest to zero distance, while the opposite condition is true for the values with the highest distance.

Results were obtained within the sliding window framework. For this purpose, the subset of a series (window), for which there were calculated entropy measures, was selected. Then, the window was displaced along the time series in a Δw increment (in our case, $\Delta w = 1$), and the procedure was repeated until all the studied series had been exhausted. During the experiments, we have found that the window size $w = 250$ days represents the change of complexity for the studied crashes in the most correct way.

Further, by comparing the dynamics of the actual time series and the corresponding measures of complexity, we can judge the characteristic changes in the dynamics of the behavior of complexity with changes in the stock index. If the constructed measure of complexity behaves in a definite way for all periods of crashes, for example, decreases or increases during the pre-critical period, then it can serve as an indicator or precursor of such crash phenomenon [9-11, 82-86].

Shannon entropy

Shannon entropy (ShEn), founded by Claude Shannon [77], is the average (expected) amount information that we can get from an event. This quantity is expressed through the probability of a random variable X and its amount of information $I(X) = -\ln p(X)$, and can be defined as

$$\mathrm{ShEn}(X) = -\sum_{i=1}^{N} p(x_i) \ln p(x_i), \tag{6}$$

where $p(x_i)$ is the probability of occurring the value x_i of random variable X, and $\ln p(x_i)$ defines the amount of information conveyed in x_i.

In Fig. 2 is presented the dynamics of the classic ShEn calculated for the studied crashes.

In Fig. 2 we can see that during the crash period the dynamics of the classic ShEn begins to decline, indicating a decrease in the average amount of information that these events represent. This gives

us an idea that the returns of these events are distributed more ununiformly, i.e., there are a fraction of returns that are more probable compared to others.

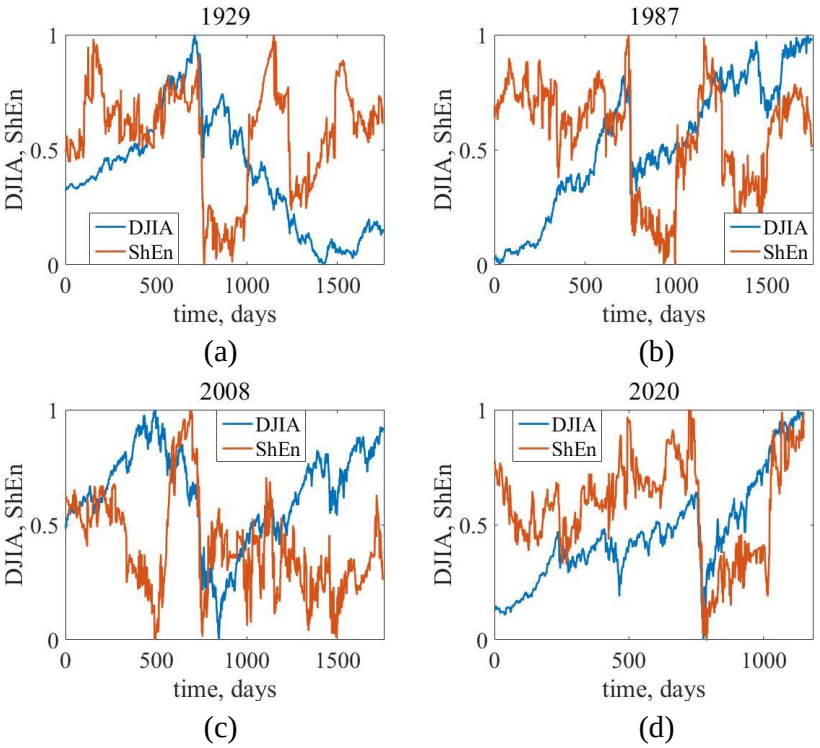

Fig. 2. The dynamics of the classic ShEn along with the crashes of 1929 (a), 1987 (b), 2008 (c), and 2020 (d) in the DJIA index

Fuzzy Shannon entropy

The measure of fuzzy information gained from a fuzzy system is known as fuzzy entropy. Compared to the classic ShEn, fuzzy entropy does not rely on a probabilistic concept since it is based on the concept of membership function $\mu(x) \in [0,1]$, which quantifies the degree of membership of a particular element x to a set. In a similar way to the ShEn, fuzzy Shannon entropy (FuzzShEn) can define how complex is presented to be the studied fuzzy set A.

Lotfi Zadeh, the founder of fuzzy set theory [99], proposed to quantify the uncertainty of a fuzzy event as a weighted ShEn, where the membership values are regarded as weights [17]:

$$\mathrm{FuzzShEn}(X) = -K \sum_{i=1}^{N} \mu(x_i) \ln \mu(x_i), \tag{7}$$

where $\mu(x_i) \in [0,1]$ is the value obtained from fuzzy membership function, and K is a positive constant (in our case, $K = 1$).

In Fig. 3 are presented the results of the FuzzShEn, according to Zadeh, calculated with the default exponential function (3) for the studied crashes.

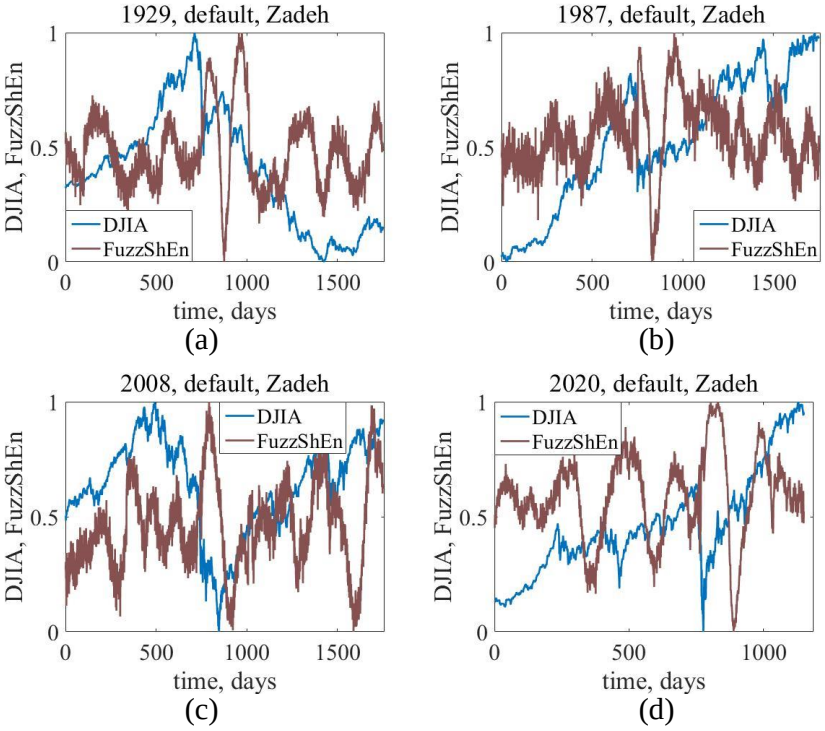

Fig. 3. The dynamics of the FuzzShEn calculated according to equation (7) with the default exponential function along with the crashes of 1929 (a), 1987 (b), 2008 (c), and 2020 (d) in the DJIA index

In Fig. 3 we see that the behavior of the FuzzShEn according to Zadeh with the default exponential function is presented as asymmetric compared to the classic ShEn. We may say that the dynamics of this indicator is lagged since the biggest decline that could be before or during the crash phenomena, appears after each crash. We could conclude that Zadeh's approach in the combination with the default function might be wrong but further improvements and experiments could be done.

In Fig. 4 is presented the FuzzShEn according to Zadeh (7) with the sigmoid membership function (4).

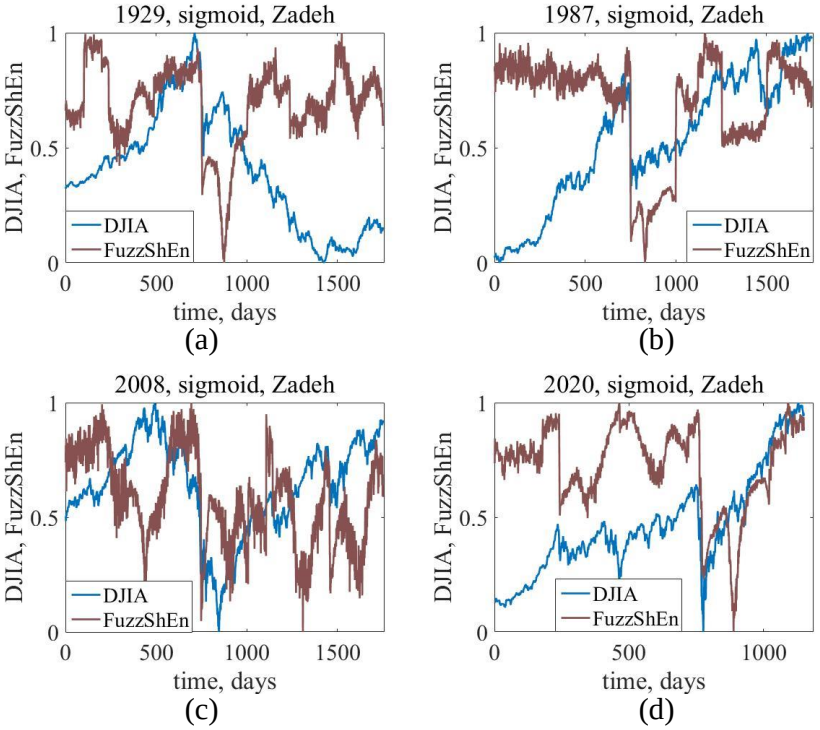

Fig. 4. The dynamics of the FuzzShEn calculated according to equation (7) with the sigmoid membership function along with the crashes of 1929 (a), 1987 (b), 2008 (c), and 2020 (d) in the DJIA index

The results presented in Fig. 4 give us an idea that the sigmoid membership function is a reasonable choice for constructing an effective indicator of crisis phenomena. According to the classic ShEn, the FuzzShEn decreases during a crisis event, indicating a decrease in the degree of randomness during this period of time. Also, the fuzzification procedure makes the presented indicator more smoothed in comparison with the classic Shannon entropy, filtering noisy oscillations in its dynamics and focusing only on the most significant crises.

In Fig. 5 is presented the FuzzShEn according to Zadeh's equation (7) with the linear membership function (5).

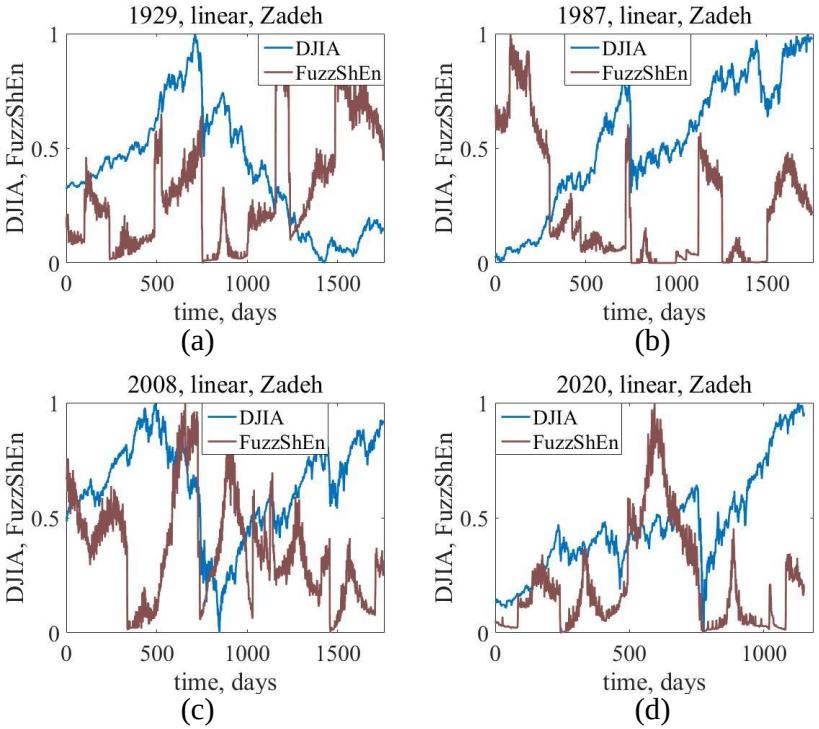

Fig. 5. The dynamics of the FuzzShEn calculated according to equation (7) with the linear membership function along with crashes of 1929 (a), 1987 (b), 2008 (c), and 2020 (d) in the DJIA index

The results in Fig. 5 illustrate that the FuzzShEn with the membership function defined in (5) became more linear. Before each crash event, our indicator starts to decline, indicating more deterministic behavior before the collapse. The studied crashes in Fig. 5 are followed by a large decrease in the dynamics of the FuzzShEn. These results are presented to be a little worse than for the sigmoid fuzzy function, but even these one gives a perspective for building effective algorithmic strategies and forecasts.

De Luca and Termini [17] suggested that the corresponding formula of entropy should be defined as

$$f(A) = H(A) + H(\bar{A}), \tag{8}$$

where $H(A)$ is a Shannon entropy of fuzzy set A, and $\bar{A}$ is its complement.

Therefore, for defining the complexity (uncertainty) of the studied system, according to De Luca and Termini, we can formulate the FuzzShEn as

$$\begin{aligned}\mathrm{FuzzShEn}(X) = -\sum_{i=1}^{N} \mu(x_i) \ln \mu(x_i) + \\ + \big(1 - \mu(x_i)\big) \ln\big(1 - \mu(x_i)\big).\end{aligned} \tag{9}$$

Standard fuzzy entropy $H(A)$ implies following conditions:

- $H(A) = 0$ if all $\mu(x_i)$ approximately equal 0 or 1;
- $H(A)$ is maximal if all $\mu(x_i)$ approximately equal to 0.5;
- $H(A) \geq H(B)$, where B is a sharpened version of A;
- $H(A) = H(\bar{A})$.

In Fig. 6 is presented the FuzzShEn according to De Luca and Termini's entropy in the combination with the default exponential membership function (3).

The results obtained in Fig. 6 according to De Luca and Termini's approach seem to be better, compared to Zadeh's entropy. Calculating it with the default exponential function some of our results demonstrate asymmetric dynamic as in Fig. 6a and Fig. 6c. However, we may see the decrease of the corresponding FuzzShEn for the crashes of 1987 (Fig. 6b) and of 2020 (Fig. 6d). Nevertheless, even

their dynamics seem to be lagged as in Zadeh's approach, and, in places, their dynamics seem to be noisier.

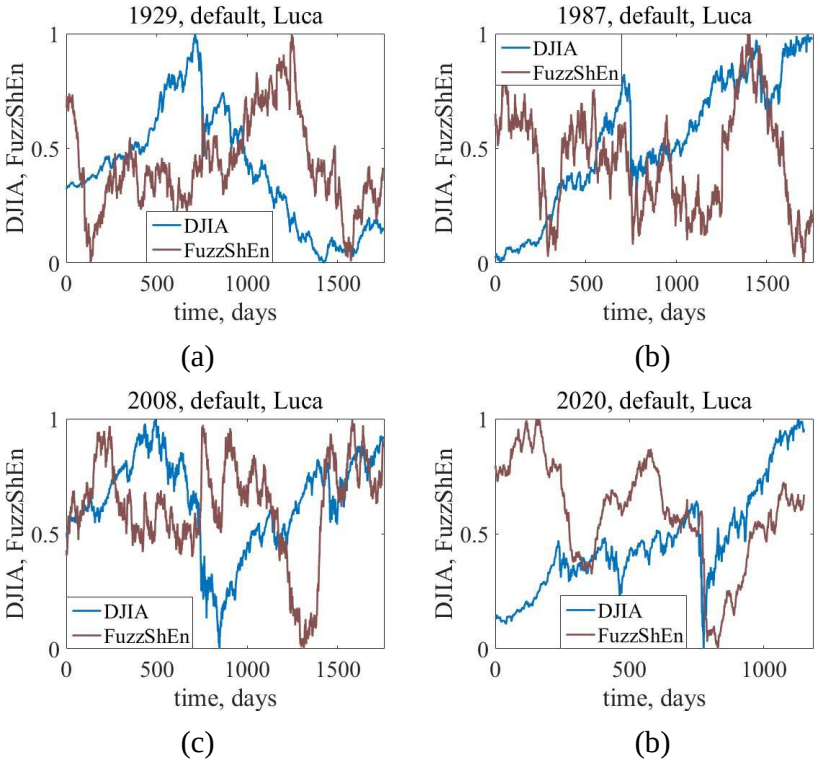

Fig. 6. The dynamics of the FuzzShEn calculated according to equation (9) with the default exponential membership function along with the crashes of 1929 (a), 1987 (b), 2008 (c), and 2020 (d) in the DJIA index

De Luca and Termini's approach in the combination with the default membership function remains as unreliable as Zadeh's FuzzShEn method.

In Fig. 7 is presented the FuzzShEn according to De Luca and Termini's entropy (9) in the combination with the sigmoid membership function (4).

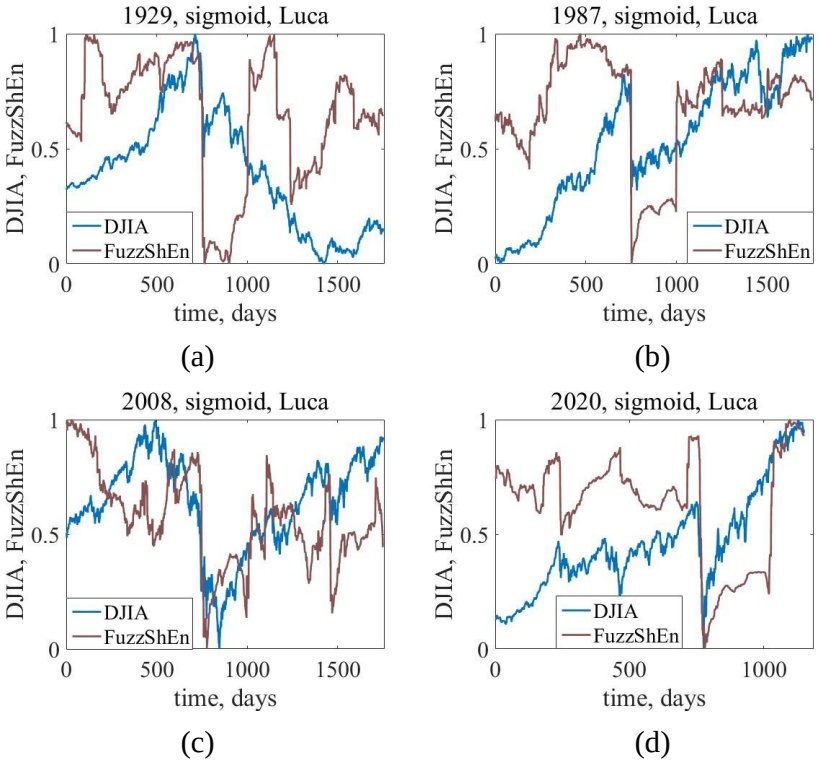

Fig. 7. The dynamics of the FuzzShEn calculated according to equation (9) with the sigmoid membership function along with the crashes of 1929 (a), 1987 (b), 2008 (c), and 2020 (d) in the DJIA index

In Fig. 7 is presented the behavior of the FuzzShEn according to De Luca and Termini. This Shannon entropy modification in combination with the sigmoid membership function gives reliable and robust results during crash events. In the case of the studied crashes, we see that the FuzzShEn is an indicator of critical phenomena rather than a precursor. With the fuzzification, it behaves smoothly and indicates the increase of persistency for all of the crashes.

Fig. 8 presents FuzzShEn (9) with the linear membership function (5).

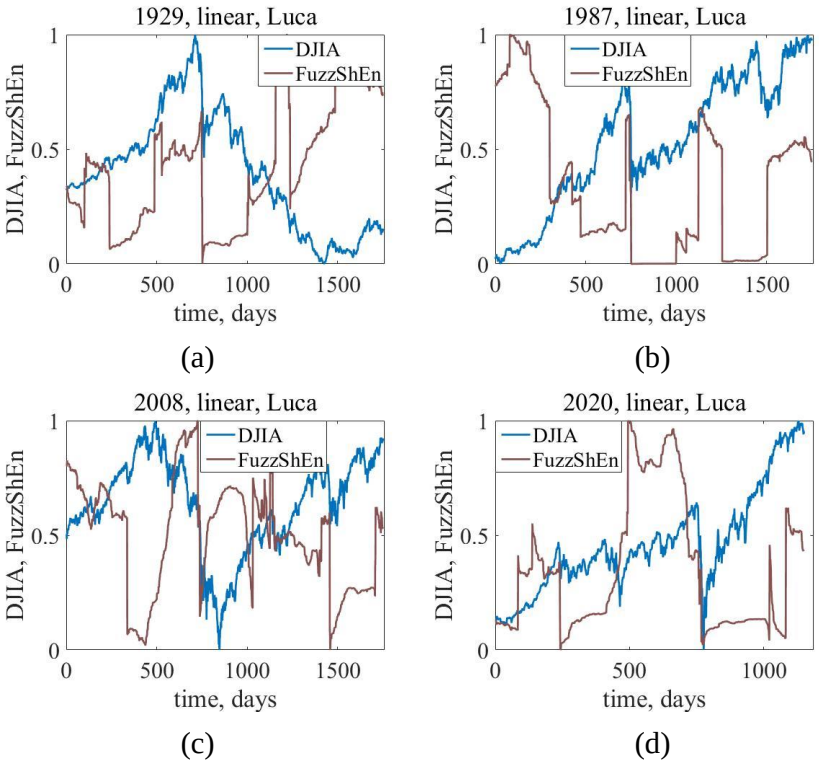

Fig. 8. The dynamics of the FuzzShEn calculated according to equation (9) with the linear membership function along with the crashes of 1929 (a), 1987 (b), 2008 (c), and 2020 (d) in the DJIA index

For this membership function, the dynamics of the FuzzShEn is also more linear. Nevertheless, the indicator starts to decline during each of the studied crashes, indicating more deterministic behavior during the collapse.

Approximate entropy

The proposed entropy allows us to quantify how regular or irregular is presented to be studied data. The idea here is to measure the likelihood that patterns in d_E-dimensional space will remain approximately the same in $d_E + 1$-dimensional space. For entropy indicators, we have chosen $d_E = 3$ and $\tau = 1$.

For step 1, we reconstruct phase space of the initial time series according to Takens' embedding theorem [91] as it is required by the procedure:

$$\vec{X}(i) = \{x(i), x(i+1), \dots, x(i+d_E-1)\}, \quad 1 \le i \le N - d_E + 1. \tag{10}$$

Then, we want to calculate how distant remain other vectors from the considered vector $\vec{X}(i)$ within the predefined threshold:

$$d\left[\vec{X}(i), \vec{X}(j)\right] = \max_{k=0,1,\dots,d_E-1} (|x(i+k) - x(j+k)|), \tag{11}$$

and for each i-th vector, we count the number of j-th vector that does not exceed the predefined radius r. In our case, $r = 0.45$, since exactly for this value this method demonstrates appropriate behavior during critical states. After counting it, we want to measure the probability of finding such vectors that will remain similar to i-th vector, where maximum absolute variation among their scalar components does not exceed the tolerance r:

$$C_i(r) = \frac{\Theta\left(r - d\left[\vec{X}(i), \vec{X}(j)\right]\right)}{N - d_E + 1}, \tag{12}$$

where $\Theta(\cdot)$ is a Heaviside function: $\mathbb{R} \to (0, 1)$.

After it, we define the mean value of $C_i(r)$:

$$\varphi^{d_E}(r) = \frac{\sum_{i=1}^{N-d_E+1} \ln C_i(r)}{N - d_E + 1}, \tag{13}$$

and the likelihood of patterns in d_E-dimensional space to remain the same in $d_E + 1$-dimensional space can be expressed using the following equation:

$$\mathrm{ApEn}\left(\vec{X}, d_E, r\right) = \varphi^{d_E}(r) - \varphi^{d_E+1}(r). \tag{14}$$

Despite ApEn usability in different fields of science, it is strongly dependent on the signal length and biased statistics due to the concavity of the logarithm function and self-matches when we

compute $C_i(r)$ [64-66]. Also, ApEn can provide unexpected variations for different r and d_E [13, 65].

Fuzzy modification of ApEn that includes membership degree overcome such cases.

In Fig. 9 are illustrated results of the classic ApEn for the studied DJIA crashes.

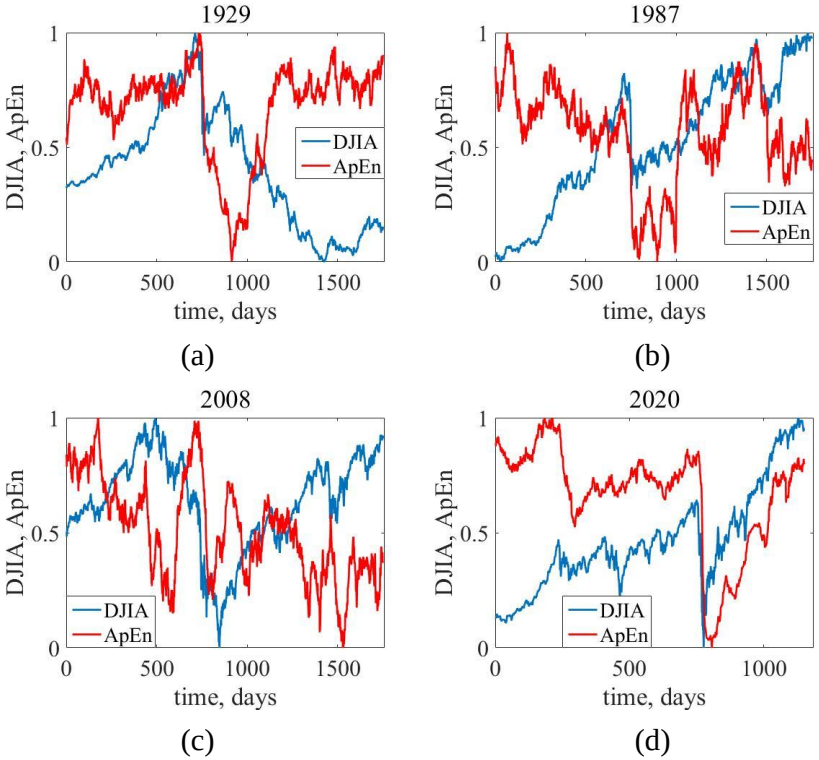

Fig. 9. The dynamics of the classic ApEn along with crashes of 1929 (a), 1987 (b), 2008 (c), and 2020 (d) in the DJIA index

The interpretation of the classic ApEn is similar to the ShEn: with the higher degree of predictability (persistency), the values of ApEn become lower. That is, with the higher probability of two trajectories in the phase-space remaining close to each other, we expect this indicator to decrease. This behavior is true for crisis events, which is confirmed by the presented results.

Fuzzy approximate entropy

After Shannon presented his entropy as a basis of information theory, different modifications have been proposed. One of them is Fuzzy Approximate Entropy (FuzzApEn). This approach excludes self-similarity between studied vectors, and instead Heaviside function that produces either 0 or 1 for similar vectors, it adopts a fuzzy membership function, which in the case of the FuzzApEn will associate the similarity between two vectors with a real value within range $[0, 1]$.

The difference can be seen on the stage of embedded matrix construction, where for the constructed embedded vectors we remove the baseline trend:

$$\vec{X}(i) = [x(i), x(i+1), \dots, x(i+d_E-1)] - x_0(i), \quad i = 1, \dots, N - d_E + 1, \tag{15}$$

where $x_0(i) = \frac{1}{d_E}\sum_{j=0}^{d_E-1} x(i+j)$. Then, the distance between each consecutive embedded vector is computed as

$$d\left[\vec{X}(i), \vec{X}(j)\right] = \max\left|\vec{X}(i) - \vec{X}(j)\right|, \quad i \geq 1, j \leq N - d_E + 1. \tag{16}$$

In the original approximate entropy, the degree of similarity between two vectors is expressed through Heaviside function. Fuzzy modification uses a membership function for measuring the distance between trajectories i and j: $D_{i,j} = \mu\left(d\left[\vec{X}(i), \vec{X}(j)\right]\right)$. Then the function φ^{d_E} is calculated as

$$\varphi^{d_E} = \frac{1}{(N - d_E + 1)} \sum_{i=1}^{N-d_E+1} \left(\frac{1}{(N - d_E)} \sum_{j=1, j\neq i}^{N-d_E} D_{i,j} \right). \tag{17}$$

Finally,

$$\text{FuzzApEn}\left(\vec{X}, d_E\right) = -[\ln \varphi^{d_E+1} - \ln \varphi^{d_E}]. \tag{18}$$

Fig. 10 presents the results of the FuzzApEn calculations for the studied crash with the usage of the default exponential function.

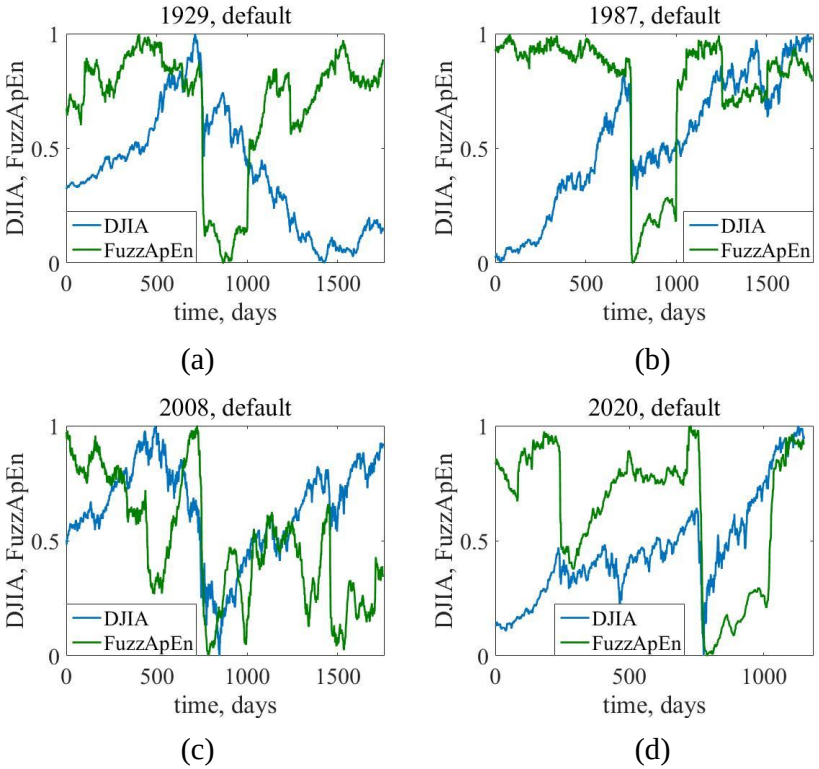

Fig. 10. The dynamics of the FuzzApEn calculated with the default exponential membership function along with the crashes of 1929 (a), 1987 (b), 2008 (c), and 2020 (d) in the DJIA index

In Fig. 10, compared to the classic ApEn, the FuzzApEn method demonstrates a similar pattern for critical events. We can see that the fuzzy indicator based on the default exponential membership function shows a significant decrease during the crash events. Moreover, it seems to be more robust to the time series length (time localization) and the choice of the parameters of the model. We have found that despite the chosen parameters r_1 and r_2 in equation (3), this indicator does not change seriously despite different combinations of the mentioned variables.

In Fig. 11 are presented the results of the FuzzApEn in the combination with the sigmoid membership function.

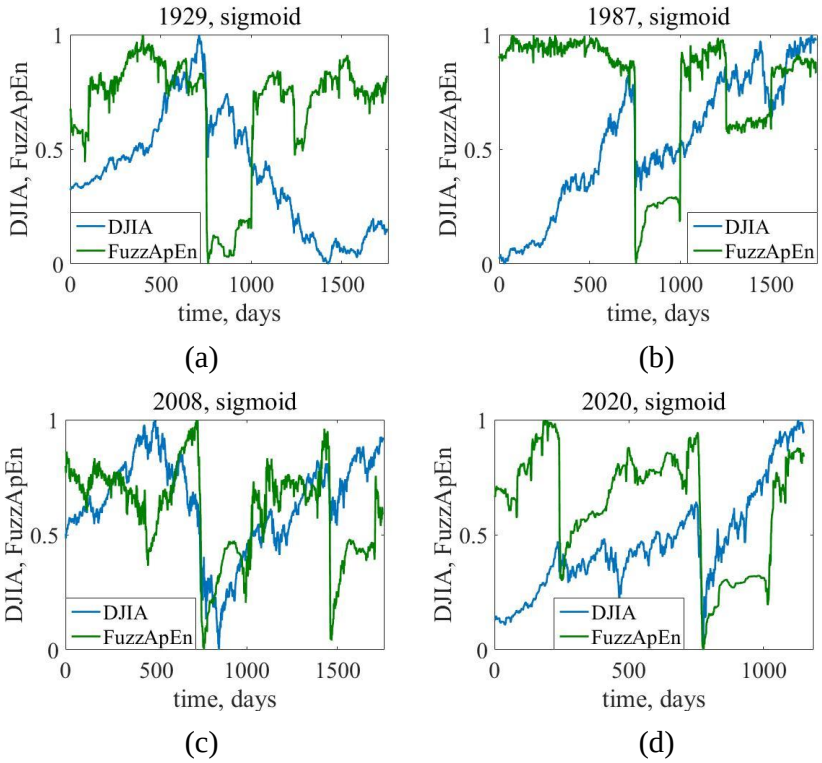

Fig. 11. The dynamics of the FuzzApEn calculated with the sigmoid membership function along with the crashes of 1929 (a), 1987 (b), 2008 (c), and 2020 (d) in the DJIA index

The results presented in Fig. 11 look identical to those from Fig. 10. During crash events the FuzzApEn declines rapidly, indicating the rise of similarity during the evolution of the trajectories in the phase-space.

The calculations of the FuzzApEn of the last membership function are presented in Fig. 12.

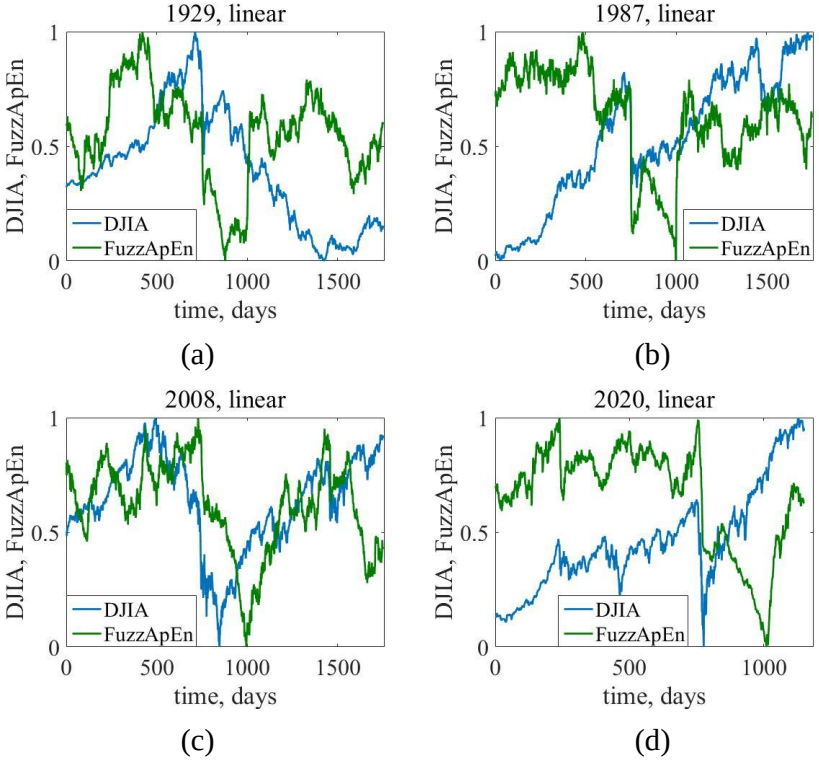

Fig. 12. The dynamics of the FuzzApEn calculated with the linear membership function along with the crashes of 1929 (a), 1987 (b), 2008 (c), and 2020 (d) in the DJIA index

Fig. 12 presents the results of the FuzzApEn for the linear membership function. The crashes of both 1929 and 1987 years according to this approach are identified in advance with the FuzzApEn. In Figs. 12a and 12b, the FuzzApEn declines before the crash, indicating more determined dynamics before crash appears to be. The results in Fig. 12c are presented to be not as reliable as the previous figures. The dynamics of the FuzzApEn for this crash demonstrates a less precuring signal compared to previous results. In this case, the behavior of the indicator looks shifted from the studied crisis, if we focus on the largest drop in entropy.

Permutation entropy

As in previous types of entropy, we reconstruct the time series of N values and a fixed embedding dimension d_E and time delay τ, forming the embedded matrix we form temporal vector sequences

$$\vec{X}(i) = \{x(i), x(i+1), \dots, x(i+[d_E-1]\tau)\}, \tag{19}$$

where $N - [d_E - 1]\tau$ vectors are obtained.

Then, each element of $\vec{X}(i)$ is transformed into numeric ranks according to their order. As an example, for $d_E = 2$ and $\tau = 1$, and time series $\vec{X} = (-0.1, 0.4, 3.2, 12.0, 6.5)$, embedded matrix will have the following pairs: $\vec{X}(1) = \{-0.1, 0.4\}$, $\vec{X}(2) = \{0.4, 3.2\}$, $\vec{X}(3) = \{3.2, 12.0\}$, $\vec{X}(4) = \{12.0, 6.5\}$.

Next, we form ordinal sequences according to their numerical order. Such pairs as $\vec{X}(1), \vec{X}(2), \vec{X}(3)$ satisfy $x(i) < x(i+1)$ and one pair $\vec{X}(4)$ satisfy $x(i) > x(i+1)$. According to PEn, it is possible to consider $d_E!$ possible permutations of order d_E. Following our example, there are only $2!$ considered patterns: $\pi_1 = \{0, 1\}$, $\pi_2 = \{1, 0\}$.

For each pattern, we determine its relative frequency:

$$p(\pi) = \frac{\#\{\vec{X}(i) \text{ has pattern } \pi\}}{N - [d_E - 1]\tau}. \tag{20}$$

The probability of finding π_1 is $3/4$ and of π_2 is $1/4$, i.e., we form the probability distribution $P = \{p(\pi_1), \dots, p(\pi_{d_E})\}$. Finally, the PEn can be calculated regarding classic Shannon entropy (6):

$$\mathrm{PEn}(\vec{X}, d_E) = -\sum_{i=1}^{d_E} p(\pi_i) \ln p(\pi_i). \tag{21}$$

According to our example, the PEn can be calculated as $-(3/4)\ln(3/4) - (1/4)\ln(1/4) \approx 0.56$.

In Fig. 13 there are presented results of the classic PEn calculated for the initial time series of the studied fragments.

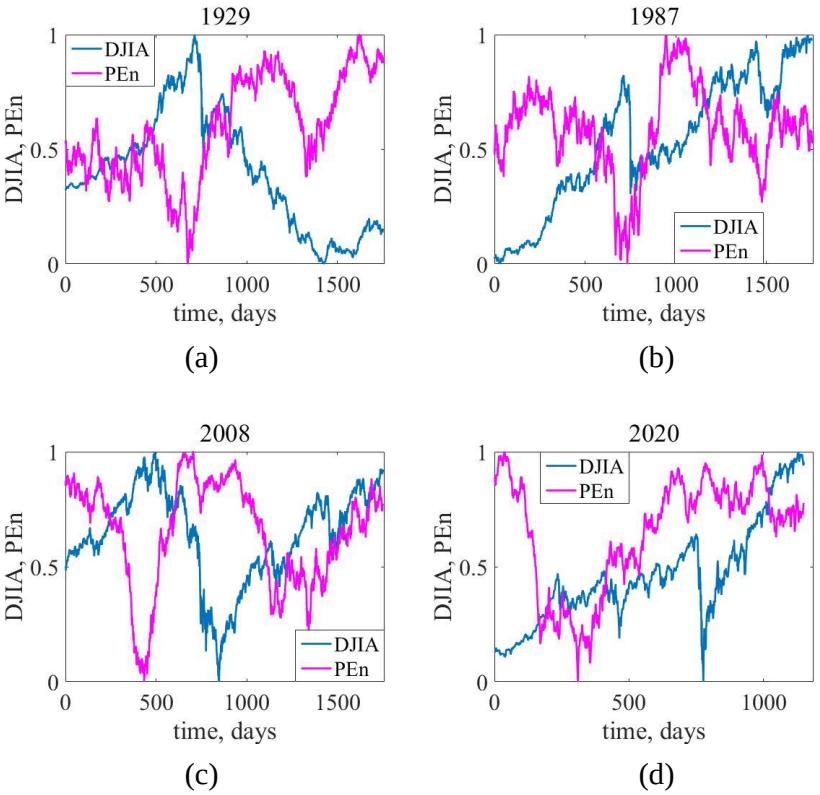

Fig. 13. The dynamics of the PEn along with the crashes of 1929 (a), 1987 (b), 2008 (c), and 2020 (d) in the DJIA index

In Fig. 13 we can see that the classic PEn appears to be the indicator precursor of the studied crashes. Long before the onset of the crisis, entropy begins to subside, indicating the extraordinary sensitivity of the series at the beginning of a particular point. This is especially evident for the 2008 crisis. In terms of the classic PEn, we may say that before the crash a particular ordinal pattern becomes more probable compared to other variants. The dynamics of the time series makes it clear that the pattern of upward dynamics ($\pi = \{0, 1, 2\}$) is more likely to occur, making the entropy values smaller.

Fuzzy permutation entropy

Similarly to the PEn, we construct the embedded matrix. Next, we need to find the distance between consecutive vectors $\vec{X}(i)$ and $\vec{X}(j)$ of the embedded matrix X. According to ApEn, we would find the largest difference between them, and if they would not exceed the predefined threshold r, we would count them.

According to the FuzzPEn, we will use another measure of distance between studied embedded vectors. In our case, we will use at least $k_0(\vec{a},\vec{b})$ number of swaps to transfer $R_{\vec{a}}$ to $R_{\vec{b}}$. For instance, if $R_{\vec{a}} = (1,2,3,5,4)$ and $R_{\vec{b}} = (5,1,2,3,4)$, then $k_0(\vec{a},\vec{b}) = 3$.

Therefore, distances are computed as

$$d\left[\vec{X}(i),\vec{X}(j)\right] = \begin{cases} k_0\left(\vec{X}(i),\vec{X}(j)\right), & j \neq i, \\ 0, & j = i. \end{cases} \tag{22}$$

At the next step each $d\left[\vec{X}(i),\vec{X}(j)\right]$ is standardized by the maximum inversion among those which are computed:

$$\overline{d_{ij}} = \frac{d\left[\vec{X}(i),\vec{X}(j)\right]}{\max\limits_{i,j}\left\{d\left[\vec{X}(i),\vec{X}(j)\right]\right\}}. \tag{23}$$

Through the fuzzy membership functions, according to (3)-(5), we calculate the similarity degree $S_{ij}^{d_E}$ for the argument $\overline{d_{ij}}$.

Next, we calculate the averages of similarity degree φ^{d_E} at states d_E:

$$\varphi^{d_E} = \frac{1}{(N-d_E+1)} \sum_{i=1}^{N-d_E+1} \frac{\sum_{j=1,i\neq j}^{N-d_E} S_{ij}^{d_E}}{N-d_E}, \tag{24}$$

and $d_E + 1$:

$$\varphi^{d_E+1} = \frac{1}{(N-d_E)} \sum_{i=1}^{N-d_E} \frac{\sum_{j=1,i\neq j}^{N-d_E-1} S_{ij}^{d_E+1}}{N-d_E-1}. \tag{25}$$

Then, the FuzzPEn is defined similarly to (18) as the difference between averaged similarity degrees at state d_E and $d_E + 1$:

$$\mathrm{FuzzPEn}\left(\vec{X}, d_E\right) = -[\ln \varphi^{d_E+1} - \ln \varphi^{d_E}]. \qquad (26)$$

In Fig. 14 there are presented the results of the FuzzPEn in the combination with the default exponential membership function.

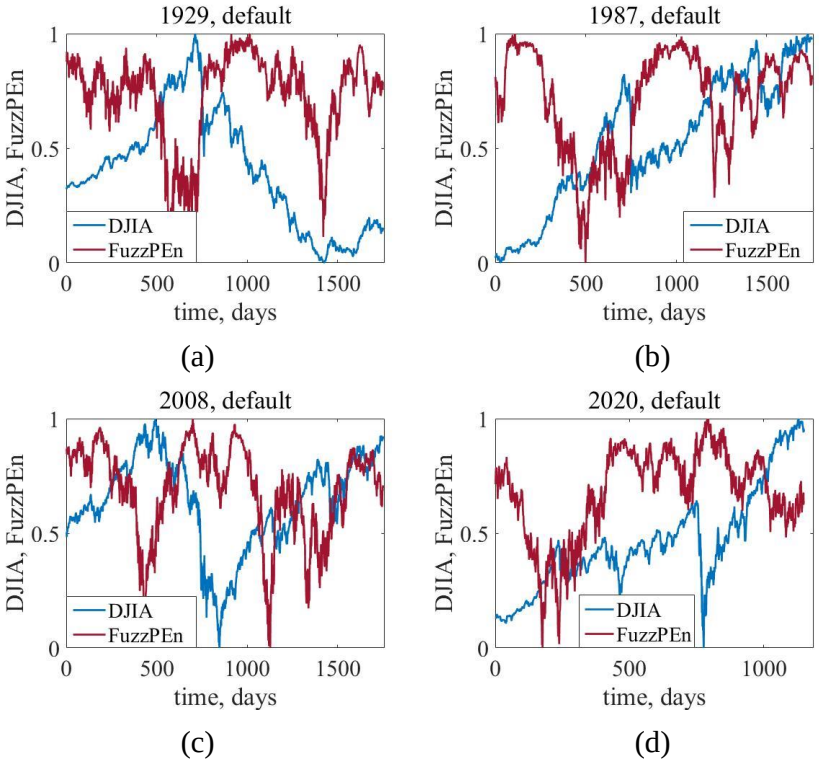

Fig. 14. The dynamics of the FuzzPEn calculated with the default exponential membership function along with the crashes of 1929 (a), 1987 (b), 2008 (c), and 2020 (d) in the DJIA index

From Fig. 14 we can see that the dynamics of this type of entropy is much more characteristic in comparison with the classic version. That is, its peak declines before the collapse are much lower and

larger. Although the behavior of classic entropy is practically indistinguishable, here fuzzification can act as an alternative to enhance the predictive effect of the indicator.

In Fig. 15 there are presented the results of the FuzzPEn in the combination with the sigmoid membership function.

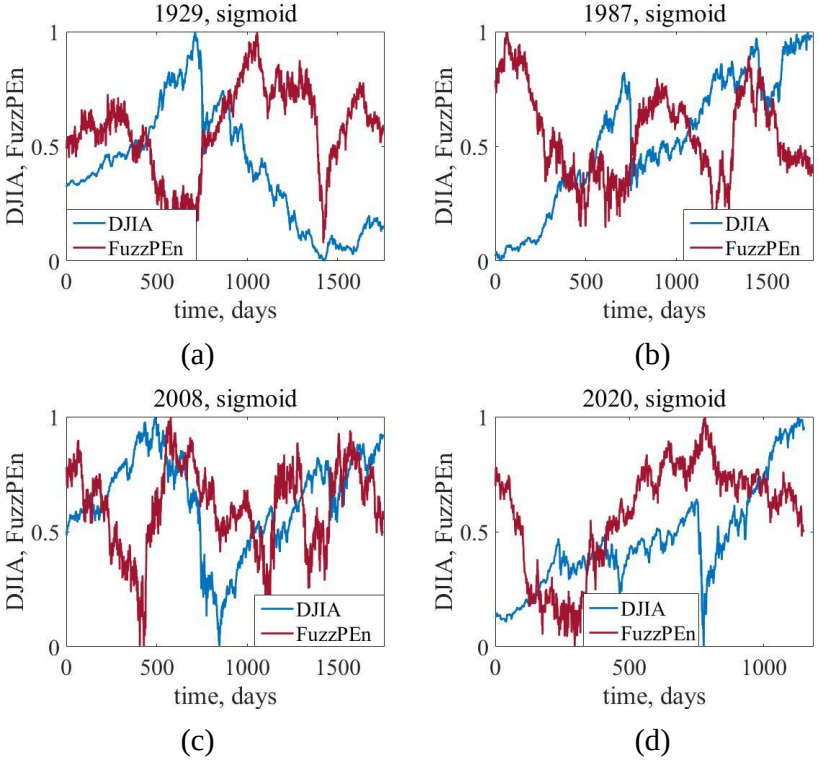

Fig. 15. The dynamics of the FuzzPEn calculated with the sigmoid membership function along with the crashes of 1929 (a), 1987 (b), 2008 (c), and 2020 (d) in the DJIA index

Fig. 15 represents similar results as for the exponential membership function. We see that each crash in the DJIA index is accompanied by a drop in the FuzzPEn. The same is true for permutation entropy with the linear membership function, as we can see in Fig. 16.

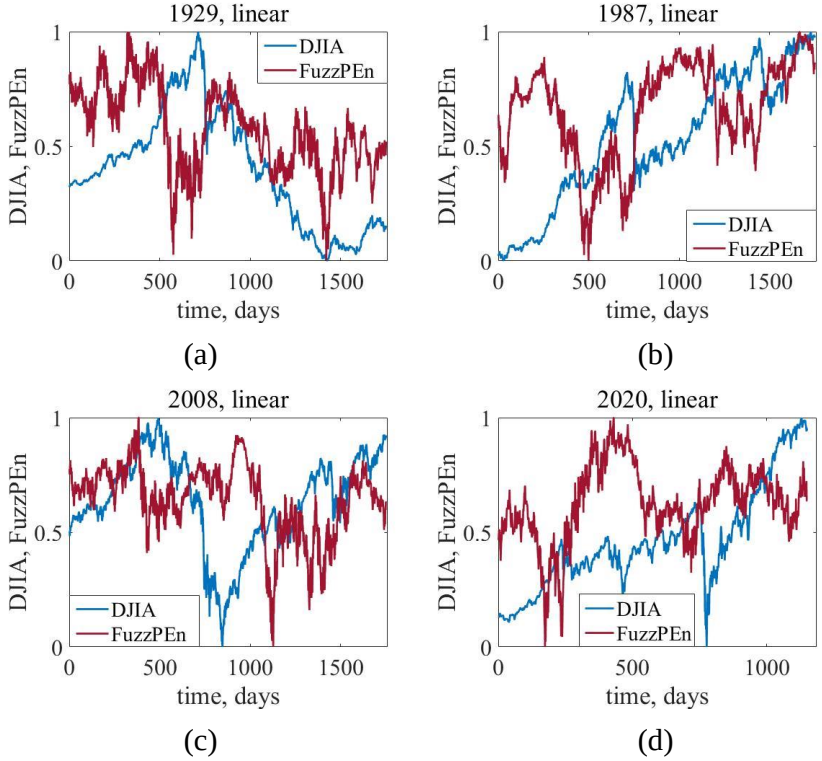

Fig. 16. The dynamics of the FuzzPEn calculated with the linear membership function along with the crashes of 1929 (a), 1987 (b), 2008 (c), and 2020 (d) in the DJIA index

As we could see, despite different membership functions, the dynamics of the FuzzPEn remains approximately the same. We could conclude that all of the membership functions would be a reasonable choice for the crisis identification and prediction regarding the FuzzPEn.

Recurrence plot and its fuzzified version

A classic recurrence plot (RP) is the representation of those states which stay close to each other or far away. Suppose we have defined $\vec{X}$ to be the set of phase states, in which $\vec{X}(i)$ is the i-th state of a

dynamical system in d_E-dimensional space. An RP is an $N \times N$ binary representation of similar or dissimilar states. On RP we put a black dot (one) if state $\vec{X}(j)$ remains within the ball of radius ε with the center $\vec{X}(i)$. This approach can be represented by the following equation:

$$R(i,j) = H\left(\varepsilon - \left\|\vec{X}(i) - \vec{X}(j)\right\|\right), \tag{27}$$

where $R(i,j)$ is an element of the recurrence matrix R, and $H(\cdot)$ is the Heaviside function that produces 1 if the relation insider brackets is positive and 0 in the opposite case.

For recurrence plots, we have set $d_E = 1$ and $\tau = 1$. Euclidian distance serves as the basis for calculating the distance between the phase-space trajectories. The threshold distance of the classic recurrence approach $\varepsilon = 0.1$.

Different patterns are formed by recurrence points: homogenous, periodic, drift, or disrupted changes. Single isolated points will occur when changes are rare. Horizontal and vertical lines indicate that the system remains in stationary states for some time, i.e., it does not change for some time or changes are very slow. Diagonal lines will indicate that the system visits the same region of the phase space at distinct times. The length of such lines represents the duration of such states.

For deterministic states, it would be more natural to have long diagonal lines and few isolated points, while for stochastic periods there would be more isolated points and short diagonal lines.

Fig. 17 presents classic RPs for the studied crashes.

As we can see from Fig. 17, the structure of recurrence plots for the studied crashes appears to be different and inhomogeneous for each crash. This approach, thanks to its visual representation, can already provide us with an understanding of how different circumstances influence the recurrent nature of each crisis, despite the visual similarity of each crash. Each RP gives an idea that the studied crashes are highly nonstationary and classical linear approaches may not be suitable for modeling the dynamics of the DJIA index. The approach based on recurrent diagrams, like the entropy methods, is sensitive to the selection of the embedding dimension d_E, the time delay τ, and such a parameter as the recurrence threshold ε. The last parameter can make the visual representation too sparse or too densely

populated with recurrence points. Fuzzy recurrence plots can represent a more stable and visually informative alternative to the classical approach [58, 62].

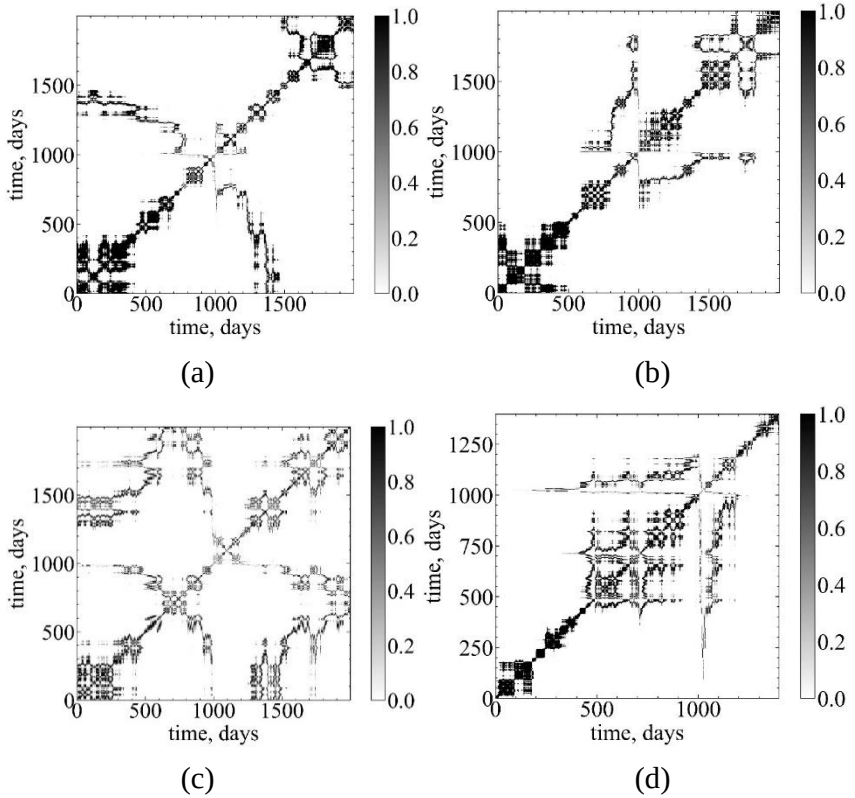

Fig. 17. Classic recurrence plots calculated for the standardized initial time fragments of the crashes of 1929 (a), 1987 (b), 2008 (c), and 2020 (d) in the DJIA index

The concept of fuzzy recurrence plot instead of simple binary representation uses similarity degree which varies between 0 and 1. In perspective, such an approach can alleviate the problem with threshold selection and enhance more detailed visualization of the studied reconstructed states.

According to this approach, in addition to the set of phase states $\vec{X}$, we define the set of fuzzy clusters $\vec{V}$ of states, respectively. A fuzzy matrix $\vec{X} \times \vec{V}$ includes the membership which defines the strength of belongingness of each pair (x, v) in R. We obtain fuzzy clusters of the phase-space using the classic fuzzy c-means (FCM) algorithm. Using this approach, we are trying to minimize the following fuzzy objective function:

$$J(M, C) = \sum_{i=1}^{N} \sum_{j=1}^{c} (\mu_{ij})^m \left[d\left(\vec{X}(i), \vec{C}(j)\right) \right]^2, \quad (28)$$

where c is the number of clusters, $1 < c < N$ (in our case, $c = 7$); $m \in [1, \infty)$ is the fuzzy weighting exponent that controls how fuzzified will be our cluster ($m = 2$ in this study); $M = \{\mu_{ij} \mid i = 1, \dots, N; j = 1, \dots, c\}$ is the matrix of the fuzzy c-partition, which is calculated according to (30); $C = \{\vec{C}(j) \mid j = 1, \dots, c\}$ is the set of cluster centers; $\vec{C}(j)$ is the fuzzy center of cluster j in d_E-dimensional space, which is calculated according to (29); $d\left(\vec{X}(i), \vec{C}(j)\right)$ is the norm metric (Euclidian distance in our case) between the phase-space trajectory $\vec{X}(i)$ and the fuzzy center $\vec{C}(j)$. Phase-space trajectories are reconstructed with the same d_E and τ as for the classic recurrence approach.

Each of the studied points *i* has a set of coefficients μ_{ij} that define their degree of belongingness to the *j*-th cluster. Each of the constructed clusters is characterized by a center $\vec{C}(j)$, which can be computed as

$$\vec{C}(j) = \frac{\sum_{i=1}^{N} (\mu_{ij})^m \vec{X}(i)}{\sum_{i=1}^{N} (\mu_{ij})^m}, \quad (29)$$

and μ_{ij} is computed as

$$\mu_{ij} = 1 \Big/ \sum_{k=1}^{c} \left[\frac{d\left(\vec{X}(i), \vec{C}(j)\right)}{d\left(\vec{X}(i), \vec{C}(k)\right)} \right]^{2/(m-1)}, 1 \le j \le c. \quad (30)$$

We stop to update the membership values μ_{ij} when $\|M^t - M^{t+1}\| \leq \varepsilon$ (in our case, $\varepsilon = 0.0001$).

Fig. 18 presents the recurrence structure of the studied crashes in terms of the fuzzy recurrence plots.

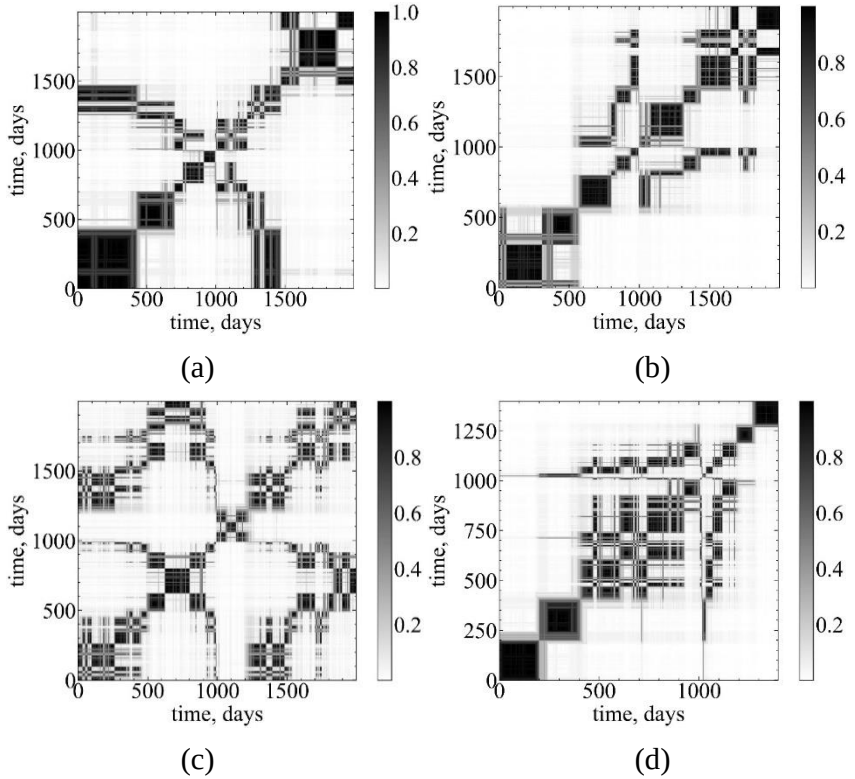

Fig. 18. Fuzzy recurrence plots calculated for the standardized returns of the crashes of 1929 (a), 1987 (b), 2008 (c), and 2020 (d) in the DJIA index

In general, FRPs present approximately the same information about each crash as the classic approach. We can see how the combination of horizontal, vertical, and diagonal structures changes across time. From the visual representation, we may conclude that the overall degree of recurrence becomes higher during critical states.

Compared to the classic method, there are very little amount of isolated points in this type of diagram. Relying on fuzzy clustering, we get more squared and densely populated recurrence points that, in some way, make fuzzy recurrence representation more informative compared to the classic one.

Conclusions

The existing literature devoted to the study of complex nonlinear systems with the usage of fuzzy modifications gives an understanding that the theory of fuzzy logic will get its further development over many years. Different areas of science show that the theory of fuzzy sets is especially efficient when dealing with uncertainty and vagueness. Moreover, in the future, the development of fuzzy set theory in combination with information theory, chaos theory, non-extensive Tsallis statistics, irreversibility theory, theory of complex networks, etc. is no less interesting.

In this study, for the first time, we have presented indicators (indicators-precursors) based on fuzzy entropy theory and fuzzy recurrence plots. Here, we have performed a comparative analysis of both classic methods and their fuzzy analogs. For the benchmark of our analysis, we have chosen the Dow Jones Industrial Index, as it is one of the most capitalized and commonly followed financial indicator in the world. Following the list of stock market crashes and bear markets [49], we have selected four the most known crashes of the stock market as a baseline of our analysis: the crises of 1929, 1987, 2008, and 2020 years. The sub-series of crashes were obtained from the daily data of the DJIA index. The monitoring of the evolution of the market was performed with the sliding window approach.

Since information theory is currently saturated with various entropy indicators, as a starting point for further research on the theory of fuzzy sets, we took the classical Shannon, approximate, and permutation entropies, and their fuzzy alternatives – fuzzy Shannon, approximate, and permutation entropy. Each of the fuzzy modifications was accompanied by three fuzzy membership functions: default exponential fuzzy function, sigmoid fuzzy function, and simple linear function. All of the empirical results show that the fuzzification of the original entropy approaches gives great

perspectives to the construction of the effective and robust indicators (indicators-precursors) of critical events in the studied complex systems. Experimenting with the different time window of different sizes, threshold parameters, embedding dimension, and time delays, we have approved that fuzzy entropies are stable to the length of the time series, embedding dimension, delay, and threshold parameters, compared to the classic approaches. We have found that the sigmoid membership function is the leading variant among the proposed. Although other fuzzy functions demonstrated perfect results, for example, for the FuzzApEn or the FuzzPEn, there still remains a problem with the FuzzShEn. Also, some of the presented crashes could not be identified as good as with the usage of the sigmoid approach. In our opinion, this type of function has to be leading during the construction of the trading strategies based on fuzzy entropies.

Precisely the same conclusion could be done for fuzzy recurrence plots. In addition, this paper presents a comparative analysis of classical and fuzzy recurrent diagrams. In general, FRPs presented precisely the same amount of information about each crash as the classic approach. Compared to the classic method, the structure of that type of RP appeared to be more inhomogeneous. Relying on fuzzy clustering, we have gotten more squared and densely populated recurrence points that, in some way, made fuzzy recurrence representation more informative compared to the classic one. Further, it would be interesting to present indicators of crash events based on fuzzy cross-recurrence plots, fuzzy recurrence network, fuzzy recurrence quantification analysis, and fuzzy recurrence entropies, combining it all with the deep learning approaches [59, 60, 61, 63, 87].

The proposed econophysics approaches demonstrate promising results not only for researchers but also for practitioners: ordinary investors, professional traders, and data analysts. The prospective of using fuzzy-based approaches is not limited only by the construction of indicators for trading, but also, they can be applied to banking regulation, portfolio management, and financial forecasting [75].

References

1. Acharya, U.R., Sree, S.V., Chattopadhyay, S., Yu, W., & Ang, P.C.A. (2011). Application of recurrence quantification analysis for the automated

identification of epileptic EEG signals. *International journal of neural systems*, *21*(03), 199-211. https://doi.org/10.1142/s0129065711002808

2. Aldalou, E., & Perçin, S. (2020). Application of integrated fuzzy MCDM approach for financial performance evaluation of Turkish technology sector. *International Journal of Procurement Management*, *13*(1), 1-23. https://doi.org/10.1504/ijpm.2020.105198

3. Al-Sharhan, S., Karray, F., Gueaieb, W., & Basir, O. (2001). Fuzzy entropy: a brief survey. In *Proceedings of the 10th IEEE international conference on fuzzy systems (Cat. No. 01CH37297): Vol. 3* (pp. 1135-1139). IEEE. https://doi.org/10.1109/FUZZ.2001.1008855

4. Alves, P. (2019). Chaos in historical prices and volatilities with five-dimensional Euclidean spaces. *Chaos, Solitons & Fractals: X*, *1*, Article 100002. https://doi.org/10.1016/j.csfx.2019.100002

5. Argyroudis, G. S., & Siokis, F. M. (2019). Spillover effects of Great Recession on Hong-Kong's Real Estate Market: An analysis based on Causality Plane and Tsallis Curves of Complexity–Entropy. *Physica A: Statistical Mechanics and its Applications*, *524*, 576–586. https://doi.org/10.1016/j.physa.2019.04.052

6. Azami, H., Fernández, A., & Escudero, J. (2017). Refined multiscale fuzzy entropy based on standard deviation for biomedical signal analysis. *Medical & Biological Engineering & Computing*, *55*(11), 2037–2052. https://doi.org/10.1007/s11517-017-1647-5

7. Bandt, C., & Pompe, B. (2002). Permutation Entropy: A Natural Complexity Measure for Time Series. *Physical Review Letters*, *88*(17), Article 174102. https://doi.org/10.1103/physrevlett.88.174102

8. Bastos, J. A., & Caiado, J. (2011). Recurrence quantification analysis of global stock markets. *Physica A: Statistical Mechanics and its Applications*, *390*(7), 1315–1325. https://doi.org/10.1016/j.physa.2010.12.008

9. Bielinskyi, A., Semerikov, S., Serdyuk, O., Solovieva, V., Soloviev, V., & Pichl, L. (2020). Econophysics of sustainability indices. *CEUR Workshop Proceedings*, *2713*, 372-392. http://ceur-ws.org/Vol-2713/paper41.pdf

10. Bielinskyi, A., & Soloviev, V. (2018). Complex network precursors of crashes and critical events in the cryptocurrency market. *CEUR Workshop Proceedings*, *2292*, 37-45. http://ceur-ws.org/Vol-2292/paper02.pdf

11. Bielinskyi, A., Soloviev, V., Semerikov, S., & Solovieva, V. (2019). Detecting stock crashes using Levy distribution. *CEUR Workshop Proceedings*, *2422*, 420-433. http://ceur-ws.org/Vol-2422/paper34.pdf

12. Boccara, N. (2010). *Modeling complex systems*. Springer Science & Business Media. https://doi.org/10.1007/978-1-4419-6562-2

13. Castiglioni, P., & Di Rienzo, M. (2008). How the threshold "r" influences approximate entropy analysis of heart-rate variability. In

Proceedings of the 2008 Computers in Cardiology (pp. 561-564). IEEE. https://doi.org/10.1109/CIC.2008.4749103

14. Chen, W., Wang, Z., Xie, H., & Yu, W. (2007). Characterization of Surface EMG Signal Based on Fuzzy Entropy. *IEEE Transactions on Neural Systems and Rehabilitation Engineering*, *15*(2), 266–272. https://doi.org/10.1109/tnsre.2007.897025

15. Chen, W., Zhuang, J., Yu, W., & Wang, Z. (2009). Measuring complexity using FuzzyEn, ApEn, and SampEn. *Medical Engineering & Physics*, *31*(1), 61–68. https://doi.org/10.1016/j.medengphy.2008.04.005

16. Collet, P., Eckmann, J. P., & Koch, H. (1981). Period doubling bifurcations for families of maps on $\mathbb{R}^n$. *Journal of Statistical Physics*, *25*(1), 1–14. https://doi.org/10.1007/bf01008475

17. De Luca, A., & Termini, S. (1972). A definition of a nonprobabilistic entropy in the setting of fuzzy sets theory. *Information and Control*, *20*(4), 301–312. https://doi.org/10.1016/s0019-9958(72)90199-4

18. Duran, N.D., Dale, R., Kello, C.T., Street, C.N.H., & Richardson, D.C. (2013). Exploring the movement dynamics of deception. *Frontiers in Psychology*, *4*, Article 140. https://doi.org/10.3389/fpsyg.2013.00140

19. Eckmann, J. P., & Ruelle, D. (1985). Ergodic theory of chaos and strange attractors. *Reviews of Modern Physics*, *57*(3), 617–656. https://doi.org/10.1103/revmodphys.57.617

20. Eckmann, J. P., Kamphorst, S. O., & Ruelle, D. (1987). Recurrence Plots of Dynamical Systems. *Europhysics Letters*, *4*(9), 973–977. https://doi.org/10.1209/0295-5075/4/9/004

21. Elias, J., & Narayanan Namboothiri, V. N. (2013). Cross-recurrence plot quantification analysis of input and output signals for the detection of chatter in turning. *Nonlinear Dynamics*, *76*(1), 255–261. https://doi.org/10.1007/s11071-013-1124-0

22. Eroglu, D., McRobie, F. H., Ozken, I., Stemler, T., Wyrwoll, K. H., Breitenbach, S. F. M., Marwan, N., & Kurths, J. (2016). See–saw relationship of the Holocene East Asian–Australian summer monsoon. *Nature Communications*, *7*(1), Article 12929. https://doi.org/10.1038/ncomms12929

23. Farmer, J. D. (1982). Information Dimension and the Probabilistic Structure of Chaos. *Zeitschrift Für Naturforschung A*, *37*(11), 1304–1326. https://doi.org/10.1515/zna-1982-1117

24. García-Ochoa, E., González-Sánchez, J., Acuña, N., & Euan, J. (2008). Analysis of the dynamics of Intergranular corrosion process of sensitised 304 stainless steel using recurrence plots. *Journal of Applied Electrochemistry*, *39*(5), 637–645. https://doi.org/10.1007/s10800-008-9702-4

25. Gardini, L., Lupini, R., & Messia, M. G. (1989). Hopf bifurcation and transition to chaos in Lotka-Volterra equation. *Journal of Mathematical Biology*, *27*(3), 259–272. https://doi.org/10.1007/bf00275811

26. GitHub. (2021). *Complex systems measures*. https://github.com/Butman2099/Complex-systems-measures

27. GitHub. (2021). *EntropyHub: An open-source toolkit for entropic time series analysis*. https://github.com/MattWillFlood/EntropyHub

28. Graf, S. (1987). Statistically self-similar fractals. *Probability Theory and Related Fields*, *74*(3), 357–392. https://doi.org/10.1007/bf00699096

29. Grassberger, P., & Procaccia, I. (1983). Characterization of Strange Attractors. *Physical Review Letters*, *50*(5), 346–349. https://doi.org/10.1103/physrevlett.50.346

30. Grebogi, C., Ott, E., Pelikan, S., & Yorke, J. A. (1984). Strange attractors that are not chaotic. *Physica D: Nonlinear Phenomena*, *13*(1-2), 261-268. https://doi.org/10.1016/0167-2789(84)90282-3

31. Harris, P., Litak, G., Iwaniec, J., & Bowen, C. R. (2016). Recurrence Plot and Recurrence Quantification of the Dynamic Properties of Cross-Shaped Laminated Energy Harvester. *Applied Mechanics and Materials*, *849*, 95–105. https://doi.org/10.4028/www.scientific.net/amm.849.95

32. He, S., Sun, K., & Wang, R. (2018). Fractional fuzzy entropy algorithm and the complexity analysis for nonlinear time series. *The European Physical Journal Special Topics*, *227*(7), 943-957. https://doi.org/10.1140/epjst/e2018-700098-x

33. Hou, Y., Aldrich, C., Lepkova, K., Machuca, L., & Kinsella, B. (2016). Monitoring of carbon steel corrosion by use of electrochemical noise and recurrence quantification analysis. *Corrosion Science*, *112*, 63–72. https://doi.org/10.1016/j.corsci.2016.07.009

34. Humeau-Heurtier, A. (2015). The Multiscale Entropy Algorithm and Its Variants: A Review. *Entropy*, *17*(5), 3110–3123. https://doi.org/10.3390/e17053110

35. Hutchinson, J. E. (1981). Fractals and Self Similarity. *Indiana University Mathematics Journal*, *30*(5), 713-747. https://www.jstor.org/stable/24893080

36. Ishizaki, R., & Inoue, M. (2020). Analysis of local and global instability in foreign exchange rates using short-term information entropy. *Physica A: Statistical Mechanics and its Applications*, *555*, Article 124595. https://doi.org/10.1016/j.physa.2020.124595

37. Iwaniec, J., Uhl, T., Staszewski, W. J., & Klepka, A. (2012). Detection of changes in cracked aluminium plate determinism by recurrence analysis. *Nonlinear Dynamics*, *70*(1), 125–140. https://doi.org/10.1007/s11071-012-0436-9

38. Jahanshahi, H., Yousefpour, A., Wei, Z., Alcaraz, R., & Bekiros, S. (2019). A financial hyperchaotic system with coexisting attractors: Dynamic investigation, entropy analysis, control and synchronization. *Chaos, Solitons & Fractals*, *126*, 66–77. https://doi.org/10.1016/j.chaos.2019.05.023

39. Kantz, H. (1994). A robust method to estimate the maximal Lyapunov exponent of a time series. *Physics Letters A*, *185*(1), 77–87. https://doi.org/10.1016/0375-9601(94)90991-1

40. Konvalinka, I., Xygalatas, D., Bulbulia, J., Schjødt, U., Jegindø, E. M., Wallot, S., van Orden, G., & Roepstorff, A. (2011). Synchronized arousal between performers and related spectators in a fire-walking ritual. *Proceedings of the National Academy of Sciences of the United States of America*, *108*(20), 8514–8519. https://doi.org/10.1073/pnas.1016955108

41. Lahmiri, S., & Bekiros, S. (2017). Disturbances and complexity in volatility time series. *Chaos, Solitons & Fractals*, *105*, 38–42. https://doi.org/10.1016/j.chaos.2017.10.006

42. Lahmiri, S., & Bekiros, S. (2019). Nonlinear analysis of Casablanca Stock Exchange, Dow Jones and S&P500 industrial sectors with a comparison. *Physica A: Statistical Mechanics and its Applications*, *539*, Article 122923. https://doi.org/10.1016/j.physa.2019.122923

43. Lahmiri, S., & Bekiros, S. (2020). Randomness, Informational Entropy, and Volatility Interdependencies among the Major World Markets: The Role of the COVID-19 Pandemic. *Entropy*, *22*(8), Article 833. https://doi.org/10.3390/e22080833

44. Lahmiri, S., Bekiros, S., & Avdoulas, C. (2018). Time-dependent complexity measurement of causality in international equity markets: A spatial approach. *Chaos, Solitons & Fractals*, *116*, 215–219. https://doi.org/10.1016/j.chaos.2018.09.030

45. Lahmiri, S., Uddin, G. S., & Bekiros, S. (2017). Nonlinear dynamics of equity, currency and commodity markets in the aftermath of the global financial crisis. *Chaos, Solitons & Fractals*, *103*, 342–346. https://doi.org/10.1016/j.chaos.2017.06.019

46. Lam, W. S., Lam, W. H., Jaaman, S. H., & Liew, K. F. (2021). Performance Evaluation of Construction Companies Using Integrated Entropy–Fuzzy VIKOR Model. *Entropy*, *23*(3), Article 320. https://doi.org/10.3390/e23030320

47. Li, P., Liu, C., Li, K., Zheng, D., Liu, C., & Hou, Y. (2014). Assessing the complexity of short-term heartbeat interval series by distribution entropy. *Medical & Biological Engineering & Computing*, *53*(1), 77–87. https://doi.org/10.1007/s11517-014-1216-0

48. Li, S., Zhao, Z., Wang, Y., & Wang, Y. (2011). Identifying spatial patterns of synchronization between NDVI and climatic determinants using joint recurrence plots. *Environmental Earth Sciences*, *64*(3), 851–859. https://doi.org/10.1007/s12665-011-0909-z

49. List of stock market crashes and bear markets. (2021, August 1). In *Wikipedia*. https://en.wikipedia.org/w/index.php?title=List_of_stock_market_crashes_and_bear_markets

50. Longwic, R., Litak, G., & Sen, A. K. (2009). Recurrence Plots for Diesel Engine Variability Tests. *Zeitschrift Für Naturforschung A*, *64*(1–2), 96–102. https://doi.org/10.1515/zna-2009-1-214

51. Mandelbrot, B. B. (1985). Self-Affine Fractals and Fractal Dimension. *Physica Scripta*, *32*(4), 257–260. https://doi.org/10.1088/0031-8949/32/4/001

52. Marwan, N., Trauth, M. H., Vuille, M., & Kurths, J. (2003). Comparing modern and Pleistocene ENSO-like influences in NW Argentina using nonlinear time series analysis methods. *Climate Dynamics*, *21*(3–4), 317–326. https://doi.org/10.1007/s00382-003-0335-3

53. Marwan, N., Wessel, N., Meyerfeldt, U., Schirdewan, A., & Kurths, J. (2002). Recurrence-plot-based measures of complexity and their application to heart-rate-variability data. *Physical Review E*, *66*(2), Article 026702. https://doi.org/10.1103/physreve.66.026702

54. Moore, J. M., Corrêa, D. C., & Small, M. (2018). Is Bach's brain a Markov chain? Recurrence quantification to assess Markov order for short, symbolic, musical compositions. *Chaos: An Interdisciplinary Journal of Nonlinear Science*, *28*(8), Article 085715. https://doi.org/10.1063/1.5024814

55. Nair, V., & Sujith, R. I. (2013). Identifying homoclinic orbits in the dynamics of intermittent signals through recurrence quantification. *Chaos: An Interdisciplinary Journal of Nonlinear Science*, *23*(3), Article 033136. https://doi.org/10.1063/1.4821475

56. Nichols, J., Trickey, S., & Seaver, M. (2006). Damage detection using multivariate recurrence quantification analysis. *Mechanical Systems and Signal Processing*, *20*(2), 421–437. https://doi.org/10.1016/j.ymssp.2004.08.007

57. Palmieri, F., & Fiore, U. (2009). A nonlinear, recurrence-based approach to traffic classification. *Computer Networks*, *53*(6), 761–773. https://doi.org/10.1016/j.comnet.2008.12.015

58. Pham, T. D. (2016). Fuzzy recurrence plots. *Europhysics Letters*, *116*(5), Article 50008. https://doi.org/10.1209/0295-5075/116/50008

59. Pham, T. D. (2019). Fuzzy weighted recurrence networks of time series. *Physica A: Statistical Mechanics and its Applications*, *513*, 409–417. https://doi.org/10.1016/j.physa.2018.09.035

60. Pham, T. D. (2020). Fuzzy cross and fuzzy joint recurrence plots. *Physica A: Statistical Mechanics and its Applications*, *540*, Article 123026. https://doi.org/10.1016/j.physa.2019.123026

61. Pham, T. D. (2020). Fuzzy recurrence entropy. *Europhysics Letters*, *130*(4), Article 40004. https://doi.org/10.1209/0295-5075/130/40004

62. Pham, T. D. (2020). Fuzzy recurrence plots. In *Fuzzy Recurrence Plots and Networks with Applications in Biomedicine* (pp. 29-55). Springer. https://doi.org/10.1007/978-3-030-37530-0_4

63. Pham, T. D., Wardell, K., Eklund, A., & Salerud, G. (2019). Classification of short time series in early Parkinsons disease with deep learning of fuzzy recurrence plots. *IEEE/CAA Journal of Automatica Sinica*, *6*(6), 1306–1317. https://doi.org/10.1109/jas.2019.1911774

64. Pincus, S. M. (1991). Approximate entropy as a measure of system complexity. *Proceedings of the National Academy of Sciences of the United States of America*, *88*(6), 2297–2301. https://doi.org/10.1073/pnas.88.6.2297

65. Pincus, S. M., & Goldberger, A. L. (1994). Physiological time-series analysis: what does regularity quantify? *American Journal of Physiology-Heart and Circulatory Physiology*, *266*(4), H1643–H1656. https://doi.org/10.1152/ajpheart.1994.266.4.h1643

66. Pincus, S. M., & Huang, W. M. (1992). Approximate entropy: Statistical properties and applications. *Communications in Statistics – Theory and Methods*, *21*(11), 3061–3077. https://doi.org/10.1080/03610929208830963

67. Qian, Y., Yan, R., & Hu, S. (2014). Bearing Degradation Evaluation Using Recurrence Quantification Analysis and Kalman Filter. *IEEE Transactions on Instrumentation and Measurement*, *63*(11), 2599–2610. https://doi.org/10.1109/tim.2014.2313034

68. Rand, R., & Holmes, P. (1980). Bifurcation of periodic motions in two weakly coupled van der Pol oscillators. *International Journal of Non-Linear Mechanics*, *15*(4–5), 387–399. https://doi.org/10.1016/0020-7462(80)90024-4

69. Reinertsen, E., Osipov, M., Liu, C., Kane, J. M., Petrides, G., & Clifford, G. D. (2017). Continuous assessment of schizophrenia using heart rate and accelerometer data. *Physiological Measurement*, *38*(7), 1456–1471. https://doi.org/10.1088/1361-6579/aa724d

70. Richardson, D. C., & Dale, R. (2005). Looking to Understand: The Coupling Between Speakers' and Listeners' Eye Movements and Its Relationship to Discourse Comprehension. *Cognitive Science*, *29*(6), 1045–1060. https://doi.org/10.1207/s15516709cog0000_29

71. Richman, J. S., & Moorman, J. R. (2000). Physiological time-series analysis using approximate entropy and sample entropy. *American Journal of Physiology-Heart and Circulatory Physiology*, *278*(6), H2039–H2049. https://doi.org/10.1152/ajpheart.2000.278.6.h2039

72. Roncagliolo Barrera, P., Rodríguez Gómez, F., & García Ochoa, E. (2019). Assessing of New Coatings for Iron Artifacts Conservation by Recurrence Plots Analysis. *Coatings*, *9*(1), Article 12. https://doi.org/10.3390/coatings9010012

73. Rostaghi, M., & Azami, H. (2016). Dispersion Entropy: A Measure for Time-Series Analysis. *IEEE Signal Processing Letters*, *23*(5), 610–614. https://doi.org/10.1109/lsp.2016.2542881

74. Ruelle, D. (1981). Small random perturbations of dynamical systems and the definition of attractors. *Communications in Mathematical Physics*, *82*(1), 137–151. https://doi.org/10.1007/bf01206949

75. Sanchez-Roger, M., Oliver-Alfonso, M. D., & Sanchís-Pedregosa, C. (2019). Fuzzy Logic and Its Uses in Finance: A Systematic Review Exploring Its Potential to Deal with Banking Crises. *Mathematics*, *7*(11), Article 1091. https://doi.org/10.3390/math7111091

76. Serrà, J., Serra, X., & Andrzejak, R. G. (2009). Cross recurrence quantification for cover song identification. *New Journal of Physics*, *11*, Article 093017. https://doi.org/10.1088/1367-2630/11/9/093017

77. Shannon, C. E. (1948). A Mathematical Theory of Communication. *Bell System Technical Journal*, *27*(3), 379–423. https://doi.org/10.1002/j.1538-7305.1948.tb01338.x

78. Shao, W., & Wang, J. (2020). Does the "ice-breaking" of South and North Korea affect the South Korean financial market? *Chaos, Solitons & Fractals*, *132*, Article 109564. https://doi.org/10.1016/j.chaos.2019.109564

79. Shaw, R. (1981). Strange Attractors, Chaotic Behavior, and Information Flow. *Zeitschrift Für Naturforschung A*, *36*(1), 80–112. https://doi.org/10.1515/zna-1981-0115

80. Shi, B., Wang, L., Yan, C., Chen, D., Liu, M., & Li, P. (2019). Nonlinear heart rate variability biomarkers for gastric cancer severity: A pilot study. *Scientific Reports*, *9*(1), Article 13833. https://doi.org/10.1038/s41598-019-50358-y

81. Silva, D. F., De Souza, V. M., & Batista, G. E. (2013). Time series classification using compression distance of recurrence plots. In *Proceedings of 2013 IEEE 13th International Conference on Data Mining* (pp. 687-696). IEEE. https://doi.org/10.1109/ICDM.2013.128

82. Soloviev, V., & Belinskiy, A. (2018). Complex systems theory and crashes of cryptocurrency market. In V. Ermolayev, M. Suárez-Figueroa, V. Yakovyna, H. Mayr, M. Nikitchenko, & A. Spivakovsky (Eds.), *Communications in Computer and Information Science: Vol. 1007. Information and Communication Technologies in Education, Research, and Industrial Applications* (pp. 276-297). Springer. https://doi.org/10.1007/978-3-030-13929-2_14

83. Soloviev, V., & Belinskij, A. (2018). Methods of nonlinear dynamics and the construction of cryptocurrency crisis phenomena precursors. *CEUR Workshop Proceedings*, *2104*, 116-127. http://ceur-ws.org/Vol-2104/paper_175.pdf

84. Soloviev, V., Bielinskyi, A., & Kharadzjan, N. (2020). Coverage of the coronavirus pandemic through entropy measures. *CEUR Workshop Proceedings*, *2832*, 24-42. http://ceur-ws.org/Vol-2832/paper02.pdf

85. Soloviev, V., Bielinskyi, A., Serdyuk, O., Solovieva, V., & Semerikov, S. (2020). Lyapunov exponents as indicators of the stock market crashes. *CEUR Workshop Proceedings*, *2732*, 455-470. http://ceur-ws.org/Vol-2732/20200455.pdf

86. Soloviev, V., Bielinskyi, A., & Solovieva, V. (2019). Entropy analysis of crisis phenomena for DJIA index. *CEUR Workshop Proceedings*, *2393*, 434-449. http://ceur-ws.org/Vol-2393/paper_375.pdf

87. Soloviev, V., Serdiuk, O., Semerikov, S., & Kohut-Ferens, O. (2019). Recurrence entropy and financial crashes. *Advances in Economics, Business and Management Research*, *99*, 385-388. https://dx.doi.org/10.2991/mdsmes-19.2019.73

88. Stangalini, M., Ermolli, I., Consolini, G., & Giorgi, F. (2017). Recurrence quantification analysis of two solar cycle indices. *Journal of Space Weather and Space Climate*, *7*, Article A5. https://doi.org/10.1051/swsc/2017004

89. Stender, M., Oberst, S., Tiedemann, M., & Hoffmann, N. (2019). Complex machine dynamics: systematic recurrence quantification analysis of disk brake vibration data. *Nonlinear Dynamics*, *97*(4), 2483–2497. https://doi.org/10.1007/s11071-019-05143-x

90. Strozzi, F., ZaldíVar, J. M., & Zbilut, J. P. (2002). Application of nonlinear time series analysis techniques to high-frequency currency exchange data. *Physica A: Statistical Mechanics and its Applications*, *312*(3–4), 520–538. https://doi.org/10.1016/s0378-4371(02)00846-4

91. Takens, F. (1981). Detecting strange attractors in turbulence. In D. Rand, & L. Young (Eds.), *Lecture Notes in Mathematics: Vol. 898. Dynamical systems and turbulence, Warwick 1980* (pp. 366-381). Springer-Verlag. https://doi.org/10.1007/BFb0091924

92. Voss, A., Schroeder, R., Vallverdu, M., Cygankiewicz, I., Vazquez, R., de Luna, A. B., & Caminal, P. (2008). Linear and nonlinear heart rate variability risk stratification in heart failure patients. In *Proceedings of the 2008 Computers in Cardiology* (pp. 557-560). IEEE. https://doi.org/10.1109/CIC.2008.4749102

93. Wang, G., & Wang, J. (2017). New approach of financial volatility duration dynamics by stochastic finite-range interacting voter system. *Chaos: An Interdisciplinary Journal of Nonlinear Science*, *27*(1), Article 013117. https://doi.org/10.1063/1.4974216

94. Wang, Y., Zheng, S., Zhang, W., Wang, G., & Wang, J. (2018). Fuzzy entropy complexity and multifractal behavior of statistical physics

financial dynamics. *Physica A: Statistical Mechanics and its Applications*, *506*, 486–498. https://doi.org/10.1016/j.physa.2018.04.086

95. Webber, C. L., & Zbilut, J. P. (1994). Dynamical assessment of physiological systems and states using recurrence plot strategies. *Journal of Applied Physiology*, *76*(2), 965–973. https://doi.org/10.1152/jappl.1994.76.2.965

96. Xie, H. B., He, W. X., & Liu, H. (2008). Measuring time series regularity using nonlinear similarity-based sample entropy. *Physics Letters A*, *372*(48), 7140–7146. https://doi.org/10.1016/j.physleta.2008.10.049

97. Xie, H. B., Sivakumar, B., Boonstra, T. W., & Mengersen, K. (2018). Fuzzy Entropy and Its Application for Enhanced Subspace Filtering. *IEEE Transactions on Fuzzy Systems*, *26*(4), 1970–1982. https://doi.org/10.1109/tfuzz.2017.2756829

98. Yang, Y. G., Pan, Q. X., Sun, S. J., & Xu, P. (2015). Novel Image Encryption based on Quantum Walks. *Scientific Reports*, *5*(1), Article 7784. https://doi.org/10.1038/srep07784

99. Zadeh, L. A. (1965). Fuzzy sets. *Information and Control*, *8*(3), 338–353. https://doi.org/10.1016/S0019-9958(65)90241-X

100. Zaitouny, A., Walker, D. M., & Small, M. (2019). Quadrant scan for multi-scale transition detection. *Chaos: An Interdisciplinary Journal of Nonlinear Science*, *29*(10), Article 103117. https://doi.org/10.1063/1.5109925

101. Zbilut, J. P., & Marwan, N. (2008). The Wiener–Khinchin theorem and recurrence quantification. *Physics Letters A*, *372*(44), 6622–6626. https://doi.org/10.1016/j.physleta.2008.09.027

102. Zhang, Z., Xiang, Z., Chen, Y., & Xu, J. (2020). Fuzzy permutation entropy derived from a novel distance between segments of time series. *AIMS Mathematics*, *5*(6), 6244–6260. https://doi.org/10.3934/math.2020402

103. Zhao, H., Deng, W., Yao, R., Sun, M., Luo, Y., & Dong, C. (2017). Study on a novel fault diagnosis method based on integrating EMD, fuzzy entropy, improved PSO and SVM. *Journal of Vibroengineering*, *19*(4), 2562–2577. https://doi.org/10.21595/jve.2017.18052

104. Zhao, X., & Zhang, P. (2020). Multiscale horizontal visibility entropy: Measuring the temporal complexity of financial time series. *Physica A: Statistical Mechanics and its Applications*, *537*, Article 122674. https://doi.org/10.1016/j.physa.2019.122674

105. Zhao, Z. Q., Li, S. C., Gao, J. B., & Wang, Y. L. (2011). Identifying Spatial Patterns and Dynamics of Climate Change Using Recurrence Quantification Analysis: A Case Study of Qinghai–Tibet Plateau. *International Journal of Bifurcation and Chaos*, *21*(04), 1127-1139. https://doi.org/10.1142/s0218127411028933

106. Zhou, C., & Zhang, W. (2015). Recurrence Plot Based Damage Detection Method by Integrating T^2 Control Chart. *Entropy*, *17*(5), 2624-2641. https://doi.org/10.3390/e17052624

107. Zhou, Q., & Shang, P. (2020). Weighted multiscale cumulative residual Rényi permutation entropy of financial time series. *Physica A: Statistical Mechanics and its Applications*, *540*, Article 123089. https://doi.org/10.1016/j.physa.2019.123089

108. Zhou, R., Wang, X., Wan, J., & Xiong, N. (2021). EDM-Fuzzy: An Euclidean Distance Based Multiscale Fuzzy Entropy Technology for Diagnosing Faults of Industrial Systems. *IEEE Transactions on Industrial Informatics*, *17*(6), 4046–4054. https://doi.org/10.1109/tii.2020.3009139

109. Zolotova, N. V., & Ponyavin, D. I. (2006). Phase asynchrony of the north-south sunspot activity. *Astronomy & Astrophysics*, *449*(1), L1–L4. https://doi.org/10.1051/0004-6361:200600013

The article was submitted on 2021, August 17